Adv. Theor. Appl. Mech., Vol. 3, 2010, no. 3, 121 - 138

Critical Flow Speeds of Pipes Conveying Fluid Using the Generalized Differential Quadrature Method

Francesco Tornabene, Alessandro Marzani [1], Erasmo Viola

Dipartimento di Ingegneria delle Strutture, dei Trasporti, delle Acque, del Rilevamento, del Territorio (DISTART), Università degli Studi di Bologna, Viale Risorgimento 2, 40136 Bologna, Italy
[1] alessandro.marzani@unibo.it

Isaac Elishakoff

Department of Mechanical Engineering, Florida Atlantic University, Boca Raton, FL 33431, USA

Abstract

The aim of this study is to clarify the discrepancy regarding the critical flow speed of straight pipes conveying fluids that appears to be present in the literature by using the Generalized Differential Quadrature method. It is well known that for a given "mass of the fluid" to the "mass of the pipe" ratio, straight pipes conveying fluid are unstable by a flutter mode via Hopf bifurcation for a certain value of the fluid speed, i.e. the critical flow speed. However, there seems to be lack of consensus if for a given mass ratio the system might lose stability for different values of the critical flow speed or only for a single speed value.
In this paper an attempt to answer to this question is given by solving the governing equation following first the practical aspect related to the engineering problem and than by simply considering the mathematics of the problem. The Generalized differential quadrature method is used as a numerical technique to resolve this problem. The differential governing equation is transformed into a discrete system of algebraic equations. The stability of the system is thus reduced to an eigenvalue problem. The relationship between the eigenvalue branches and

the corresponding unstable flutter modes are shown via Argand diagram. The transfer of flutter-type instability from one eigenvalue branch to another is thoroughly investigated and discussed. The critical mass ratios, at which the transfer of the eigenvalue branches related to flutter take place, are determined.

Keywords: GDQ method, stability, flutter, critical flow speed

1. Introduction

The great interest in the dynamic behaviour of a cantilever pipe conveying fluid is attributable to its non-conservative nature. Although it is quite a simple system that can be described with straightforward mathematical model, it has much in common with the dynamic behaviour of more sophisticated structures such for example an aeroplane wing. This is one of the reasons why this subject has inspired many researchers over the last 50 years.
In general, it has been established that an initially straight pipe that conveys a fluid with a relatively low speed is stable. In other words, each disturbance applied to that pipe causes a vibration that decreases with time. It has been also found that for fluid speed values higher than a certain value (the critical flow velocity) even a small disturbance could result in a system vibration that increases with time. In latter circumstances, therefore, the system equilibrium state is referred as unstable.

The critical flow speed for a straight pipe has been found to be dependent by many factors, such the ratio between the mass of the fluid and the mass of the pipe [1,2,4,5], the viscous properties of the pipe [16,19], the boundary conditions [8], the stiffness of the pipe foundation [7] among others. A comprehensive literature on the work done in this field is given in the definitive monograph by Paidoussis [14].

In the majority of the studies it has been found that a straight cantilever pipe presents a non-monotonic critical flow speed, characterized by several jumps, for an increasing mass ratio between the fluid and the pipe from zero to one. However, there seems to be lack of consensus among researchers if for a given mass ratio the system might lose stability for different values of the critical flow speed or only for a single speed value [3].

In this study an attempt to answer to this question is given by solving the governing equation of the problem following first the practical aspect related to the engineering problem and than by considering the mathematics of the problem. In the first case the mass ratio is fixed, i.e. the mass of the fluid and the mass of pipe are established, and the speed of the fluid is increased from zero to the critical flow speed. In the second case, instead, for a fixed speed of the fluid the mass ratio is determined that corresponds to system's instability. Obviously, while the first approach could be reasonably replicated experimentally, it seems to us quite complicated to perform an experiment in which the speed of the fluid is kept constant while its mass is changing. However, since the mathematics describing the stability of the system allows to look at the problem in both ways, different

critical flow speed curves have been proposed in the past, see e.g. Refs. [3] and [16]. In this study it will be shown that both approaches are mathematically feasible, but that only one has an engineering interpretation.

The Generalized Differential Quadrature (GDQ) method is used to solve the governing differential equation in both cases. The first three authors demonstrated this approach to be powerful for solution of linear dynamic self-adjoint boundary value problems [18,20-22], as well as non-self-adjoint boundary value problems [11].

The essence of this numerical method consists in replacement of partial or total derivatives of a smooth function by a weighted sum of function values at discrete points. The weighting coefficients are not related to any special physical problem and only depend on the assumed interpolating basis functions and on the spatial distribution of the discrete points [17].

In this study, first the non-dimensional differential governing equation is obtained by considering condition of equilibrium. Then, the application of the GDQ technique leads to a system of algebraic equations and the related characteristic equation in the fluid speed and mass ratio. Finally, the two analyses that have been described above are performed; in each case one of the unknowns is chosen as a parameter to solve the eigenvalue problem.

Over the past decades many methods have been used to investigate the vibration of straight and curved pipes conveying fluids, both for linear and nonlinear vibrations [6,9,10,12,13,15,23]. However, to the authors' best knowledge this study is one of very few papers [15,23] in which the GDQ method to is applied to investigate the critical flow speeds of pipes conveying fluids.

2. Problem Formulation

Consider a horizontal cantilever pipe of length L conveying a fluid. A Cartesian (x-y-z) coordinate system is adopted, with the z-axis along the geometrical axis of the pipe and the x and y-axis coincident with the principal axes of inertia of the pipe cross-section. The fluid is flowing from the fixed end to the free end with a steady flow velocity U. In the small deflection regime, if the diameter of the pipe is sufficiently smaller than the pipe length (slender pipe), the y-z plane behaviour is governed by the following equation [8]:

$$\underbrace{EI\frac{\partial^4 v}{\partial z^4}}_{\textit{elastic}} + \underbrace{m_{\mathrm{f}}U^2\frac{\partial^2 v}{\partial z^2}}_{\textit{centrifugal}} + \underbrace{2m_{\mathrm{f}}U\frac{\partial^2 v}{\partial z\partial t}}_{\textit{Coriolis}} + \underbrace{(m_{\mathrm{f}}+m_{\mathrm{p}})\frac{\partial^2 v}{\partial t^2}}_{\textit{inertia}} = 0 \qquad (1)$$

where EI is the flexural rigidity of the pipe, m_{f} and m_{p} are the mass of the fluid and the pipe per unit length, and $v = v(z,t)$ is the deflection of the pipe along the y-axis.

In eq. (1) the first term is the elastic flexural restoring force. Since $\partial^2 v/\partial z^2 \approx 1/R$, where R is the local radius of curvature, the second term in eq. (1) corresponds to the centrifugal force of the fluid flowing with constant speed U

for a curved portion of the pipe. Similarly, the third term is recognized as being associated with the Coriolis acceleration, and the last term represents inertial effects of both pipe and fluid. The pipe is clamped at $z = 0$ and free at $z = L$.

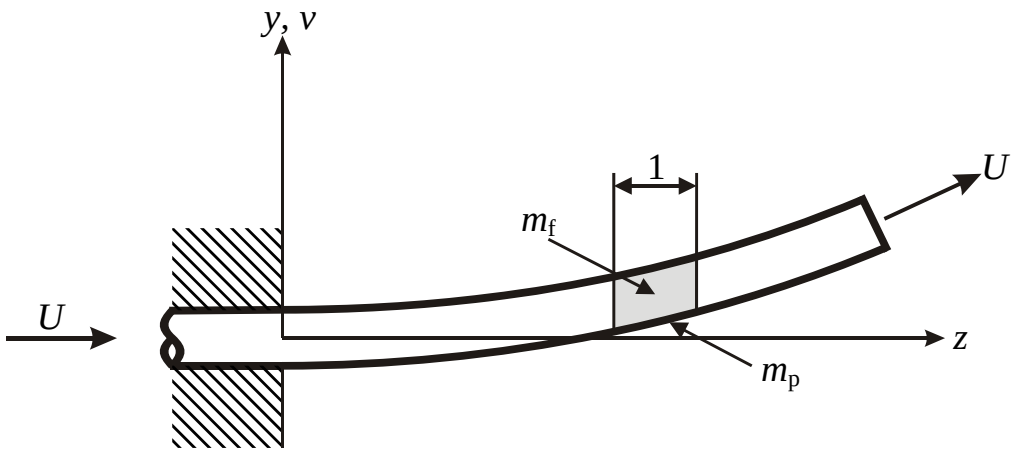

Fig. 1 - Cantilever pipe conveying fluid

The boundary conditions read:

$$v(0,t) = 0, \quad \frac{\partial v(0,t)}{\partial z} = 0 \quad at \quad z = 0 \tag{2}$$

$$\frac{\partial^2 v(L,t)}{\partial z^2} = 0, \quad \frac{\partial^3 v(L,t)}{\partial z^3} = 0 \quad at \quad z = L \tag{3}$$

We seek the solution in the form:

$$v(z,t) = V(z)e^{\Omega t} \tag{4}$$

where $V(z)$ represents the shape of the deformed configuration and Ω the circular frequency of vibration of that particular deformed configuration. Eq. (1) takes the following form:

$$EI\frac{d^4V(z)}{dz^4} + m_f U^2 \frac{d^2V(z)}{dz^2} + 2m_f U\Omega\frac{dV(z)}{dz} + (m_f + m_p)\Omega^2 V(z) = 0 \tag{5}$$

Introducing dimensionless axial coordinates $\xi = z/L$ and dividing each term of eq. (5) by the quantity EI/L^4, we get the following governing equation:

$$\frac{d^4V(\xi)}{d\xi^4} + U^2\frac{m_f L^2}{EI}\frac{d^2V(\xi)}{d\xi^2} + U\Omega\frac{2m_f L^3}{EI}\frac{dV(\xi)}{d\xi} + \Omega^2\frac{(m_f + m_p)L^4}{EI}V(\xi) = 0 \tag{6}$$

In terms of the following dimensionless parameters:

$$u = UL\sqrt{\frac{m_f}{EI}}, \quad \omega = \Omega L^2\sqrt{\frac{m_f + m_p}{EI}}, \quad \gamma = \frac{m_f}{m_f + m_p} \tag{7}$$

eq. (6) can be rewritten as:

$$\frac{d^4V(\xi)}{d\xi^4} + u^2\frac{d^2V(\xi)}{d\xi^2} + 2\omega u\sqrt{\gamma}\frac{dV(\xi)}{d\xi} + \omega^2V(\xi) = 0 \tag{8}$$

while the boundary conditions eqs. (2) and (3) are expressed as:

$$V(0) = 0, \quad \frac{dV(0)}{d\xi} = 0 \quad at \quad \xi = 0 \tag{9}$$

$$\frac{d^3V(1)}{d\xi^3} = 0, \quad \frac{d^2V(1)}{d\xi^2} = 0 \quad at \quad \xi = 1 \tag{10}$$

3. Approximate equation of motion

3.1 GDQ method review

The dimensionless differential governing equation of motion eq. (8) can be transformed into a system of algebraic equations by means of the Generalized Differential Quadrature (GDQ) method [17]. The essence of the GDQ method consists in approximating of the derivatives of the function $V(\xi)$ by a weighted sum of function values $V(\xi_i)$ at each sampling point of the discretized domain. The weighting coefficients are not related to a special problem and only depend on the derivative order and on the number and distribution (grid) of the sampling points along the domain. For example, at the ξ_i point of the domain, the *n-th* order derivative is obtained as:

$$\left.\frac{d^nV(\xi)}{d\xi^n}\right|_{\xi=\xi_i} \cong \sum_{j=1}^{N}\beta_{ij}^{(n)}V(\xi_j), \quad i = 1, 2, ..., N \tag{11}$$

where N is the total number of the sampling points of the chosen grid distribution and $\beta_{ij}^{(n)}$ are the weighting coefficients for the *n-th* order derivative at the *i-th* sampling point. The weighting coefficients can be determined once a grid points distribution has been chosen. Here, the Chebyshev-Gauss-Lobatto point distribution is assumed:

$$\xi_i = \frac{1}{2}\left[1 - \cos\left(\frac{i-1}{N-1}\pi\right)\right], \quad i = 1, 2, ..., N \tag{12}$$

The weighting coefficients are calculated by means of Lagrange interpolating functions [17]. For the first derivative, the weighting coefficients are calculated as:

$$\beta_{ij}^{(1)} = \frac{\mathsf{L}^{(1)}(\xi_i)}{(\xi_i - \xi_j)\mathsf{L}^{(1)}(\xi_j)}, \quad i, j = 1, 2, ..., N, \;\; i \neq j \tag{13}$$

$$\beta_{ii}^{(1)} = -\sum_{j=1,\, j\neq i}^{N} \beta_{ij}^{(1)}, \quad i, j = 1, 2, ..., N, \;\; i = j \tag{14}$$

while for higher order derivatives, one gets iteratively:

$$\beta_{ij}^{(n)} = n\left(\beta_{ii}^{(n-1)} \beta_{ij}^{(1)} - \frac{\beta_{ij}^{(n-1)}}{\xi_i - \xi_j} \right), \quad i \neq j, \;\; n = 2, 3, ..., N-1, \;\; i, j = 1, 2, ..., N \tag{15}$$

$$\beta_{ii}^{(n)} = -\sum_{j=1,\, j\neq i}^{N} \beta_{ij}^{(n)}, \quad i = j, \;\; n = 2, 3, ..., N-1, \;\; i, j = 1, 2, ..., N \tag{16}$$

where the first derivative of Lagrange interpolating polynomials at each point ξ_k in eq. (13) is defined as:

$$\mathsf{L}^{(1)}(\xi_k) = \prod_{l=1, l\neq k}^{N} (\xi_k - \xi_l), \quad k = 1, ..., N \tag{17}$$

It is shown in the literature that with Lagrange interpolating polynomials in conjunction with the Chebyshev-Gauss-Lobatto sampling points of eq. (12) ensures convergence, so that increasing number of sampling points *N* leads to an error decrease.

3.2 GDQ discretized governing equations

The numerical operations illustrated above in section (3.1) enable one to re-write the governing equations in discrete form, transforming every space derivative of the dependent variable into the weighted sum of node values. Thus, the differential governing equation (8) is represented via GDQ technique at the points $i = 3, 4, ..., N-2$ of the grid domain as follows:

$$\sum_{j=1}^{N} \beta_{ij}^{(4)} V_j + u^2 \sum_{j=1}^{N} \beta_{ij}^{(2)} V_j + 2\omega u \sqrt{\gamma} \sum_{j=1}^{N} \beta_{ij}^{(1)} V_j + \omega^2 V_i = 0 \tag{18}$$

while the boundary conditions eqs. (9) and (10) are expressed at the first grid point $i = 1$ ($\xi = 0$) as:

$$V_1 = 0, \quad \sum_{j=1}^{N} \beta_{1j}^{(1)} V_j = 0 \tag{19}$$

and at the last, $i = N$ grid point ($\xi = 1$), as:

$$\sum_{j=1}^{N} \beta_{Nj}^{(2)} V_j = 0, \quad \sum_{j=1}^{N} \beta_{Nj}^{(3)} V_j = 0 \tag{20}$$

Note that, remarkably, any discrete equation needs to be formulated at the grid points $i = 2$ and $i = N-1$, as proved by Shu [17]. We introduce the following notations:

$$\mathbf{B}_{ij}^{(1)} = \beta_{ij}^{(1)}, \quad \mathbf{B}_{ij}^{(2)} = \beta_{ij}^{(2)}, \quad \mathbf{B}_{ij}^{(4)} = \beta_{ij}^{(4)}, \qquad i = 3,4,...,N-2, \quad j = 1,2,...,N \tag{21}$$

representing the $(N-4)\times N$ matrices of the derivatives of the weighting coefficients; $\mathbf{I}$ denotes the $(N-4)\times(N-4)$ identity matrix. As a result, the $N-4$ field equations defined by eq. (18) can be re-written in the following matrix form:

$$\left(\mathbf{B}^{(4)} + u^2\mathbf{B}^{(2)} + 2\omega u\sqrt{\gamma}\mathbf{B}^{(1)}\right)\boldsymbol{\delta} + \omega^2\mathbf{I}\boldsymbol{\delta}_d = \mathbf{0} \tag{22}$$

In eq. (22) $\boldsymbol{\delta} = \begin{bmatrix} V_1 & V_2 & \cdots & V_{N-1} & V_N \end{bmatrix}^{\mathrm{T}}$ is the $N\times 1$ vector of unknown displacements at the grid points, whereas the vector $\boldsymbol{\delta}_d = \begin{bmatrix} V_3 & V_4 & \cdots & V_{N-4} & V_{N-3} \end{bmatrix}^{\mathrm{T}}$ collects only the $(N-4)\times 1$ unknown displacements at the domain points. The four boundary conditions described in eqs. (19)-(20) are also written in the vector notation as:

$$\mathbf{K}_b\boldsymbol{\delta} = \mathbf{0} \tag{23}$$

where the $4\times N$ matrix $\mathbf{K}_b$ is defined as:

$$\mathbf{K}_b = \begin{bmatrix} 1 & 0 & \cdots & 0 & 0 \\ \beta_{11}^{(1)} & \beta_{12}^{(1)} & \cdots & \beta_{1(N-1)}^{(1)} & \beta_{1N}^{(1)} \\ \beta_{N1}^{(3)} & \beta_{N2}^{(3)} & \cdots & \beta_{N(N-1)}^{(3)} & \beta_{1N}^{(3)} \\ \beta_{N1}^{(2)} & \beta_{N2}^{(2)} & \cdots & \beta_{N(N-1)}^{(2)} & \beta_{NN}^{(2)} \end{bmatrix} \tag{24}$$

The discrete field (22) and boundary conditions (23) can be combined into the N algebraic equations in the N unknowns nodal displacements as follows:

$$\begin{bmatrix} \mathbf{K}_b \\ \mathbf{B}^{(4)} + u^2\mathbf{B}^{(2)} + 2\omega u\sqrt{\gamma}\mathbf{B}^{(1)} \end{bmatrix}\boldsymbol{\delta} + \begin{bmatrix} \mathbf{0} \\ \omega^2\mathbf{I}\boldsymbol{\delta}_d \end{bmatrix} = \mathbf{0} \tag{25}$$

In order to calculate the natural frequencies of the structure, eq. (25) needs to be reorganized in the following form:

$$\left(\begin{bmatrix} \mathbf{K}_{bb} & \mathbf{K}_{bd} \\ \mathbf{B}_{db}^{(4)} & \mathbf{B}_{dd}^{(4)} \end{bmatrix} + u^2\begin{bmatrix} \mathbf{0} & \mathbf{0} \\ \mathbf{B}_{db}^{(2)} & \mathbf{B}_{dd}^{(2)} \end{bmatrix} + 2\omega u\sqrt{\gamma}\begin{bmatrix} \mathbf{0} & \mathbf{0} \\ \mathbf{B}_{db}^{(1)} & \mathbf{B}_{dd}^{(1)} \end{bmatrix}\right)\begin{bmatrix} \boldsymbol{\delta}_b \\ \boldsymbol{\delta}_d \end{bmatrix} + \omega^2\begin{bmatrix} \mathbf{0} & \mathbf{0} \\ \mathbf{0} & \mathbf{I} \end{bmatrix}\begin{bmatrix} \boldsymbol{\delta}_b \\ \boldsymbol{\delta}_d \end{bmatrix} = \begin{bmatrix} \mathbf{0} \\ \mathbf{0} \end{bmatrix} \tag{26}$$

where the subscripts b and d refer to the system degrees of freedom at the boundaries and in the beam domain, respectively, and $\boldsymbol{\delta}_b = \begin{bmatrix} V_1 & V_2 & V_{N-1} & V_N \end{bmatrix}^{\mathrm{T}}$. Kinematic condensation of all the non-domain degrees of freedom leads to the following equation:

$$\left(\mathbf{B}_{dd}^{(4)} - \mathbf{B}_{db}^{(4)}\mathbf{K}_{bb}^{-1}\mathbf{K}_{bd} + u^2\left(\mathbf{B}_{dd}^{(2)} - \mathbf{B}_{db}^{(2)}\mathbf{K}_{bb}^{-1}\mathbf{K}_{bd}\right) + 2\omega u\sqrt{\gamma}\left(\mathbf{B}_{dd}^{(1)} - \mathbf{B}_{db}^{(1)}\mathbf{K}_{bb}^{-1}\mathbf{K}_{bd}\right) + \omega^2\mathbf{I}\right)\boldsymbol{\delta}_d = \mathbf{0} \tag{27}$$

Finally, introducing the identity $\mathbf{I}\omega\boldsymbol{\delta}_b - \omega\mathbf{I}\boldsymbol{\delta}_b = \mathbf{0}$ the eq. (27) is transformed into a first order eigenvalue problem as follows:

$$\left(\begin{bmatrix} \mathbf{0} & \mathbf{I} \\ \mathbf{K}_d & \mathbf{K}_\omega \end{bmatrix} - \omega\begin{bmatrix} \mathbf{I} & \mathbf{0} \\ \mathbf{0} & -\mathbf{I} \end{bmatrix}\right)\begin{bmatrix} \boldsymbol{\delta}_d \\ \omega\boldsymbol{\delta}_d \end{bmatrix} = \begin{bmatrix} \mathbf{0} \\ \mathbf{0} \end{bmatrix} \tag{28}$$

where the notations have been utilized:

$$\begin{aligned} \mathbf{K}_d &= \mathbf{B}_{dd}^{(4)} - \mathbf{B}_{db}^{(4)}\mathbf{K}_{bb}^{-1}\mathbf{K}_{bd} + u^2\left(\mathbf{B}_{dd}^{(2)} - \mathbf{B}_{db}^{(2)}\mathbf{K}_{bb}^{-1}\mathbf{K}_{bd}\right) \\ \mathbf{K}_\omega &= 2u\sqrt{\gamma}\left(\mathbf{B}_{dd}^{(1)} - \mathbf{B}_{db}^{(1)}\mathbf{K}_{bb}^{-1}\mathbf{K}_{bd}\right) \end{aligned} \tag{29}$$

The dynamics of the system is well understood for the case $u > 0$. For sufficiently small u the dynamics is dominated by the Coriolis force, that is proportional to u; the system is subjected to flow-induced damping and hence stable. For increasing values of u, however, the centrifugal force, that is proportional to u^2, which may also be viewed as a compressive force, might overcome the Coriolis damping effect, and the system can lose stability by a single-mode flutter via the Hopf bifurcation. The velocity of the fluid that denotes the boundary between the stable and unstable behaviours of the system is called the critical velocity, u_{cr}. The pipe system is thus unstable if the velocity of the fluid is faster than the critical velocity.

The critical fluid velocity can thus be calculated as the velocity for which the system loses stability. Based on the assumed solution form $v(z,t) = V(z)e^{\Omega t}$, where $V(z)$ is a bounded displacement function, the stability of the system can be determined, for example, by studying sign of the complex exponent $\Omega = \mathrm{Re}\,\Omega + i\,\mathrm{Im}\,\Omega$ for increasing values of the fluid speed u. Specifically, if $\mathrm{Re}\,\Omega < 0$, the system is stable, whereas if $\mathrm{Re}\,\Omega > 0$, the system is unstable by flutter; at $\mathrm{Re}\,\Omega = 0$ the fluid is flowing at the critical flow speed. For the notation made in eq. (7), the sign of Ω is corresponding to that of the dimensionless frequency of vibration parameter ω. Therefore u_{cr} can be viewed as the critical fluid speed for which the real component of the system eigenfrequencies reaches zero value for a non-zero fluid speed.

In addition, the stability boundaries can also be obtained by looking for that particular system in terms of mass ratio γ_{cr} that presents $\mathrm{Re}\,\Omega = 0$ for a given value of the fluid speed u. In the following both procedures are examined.

4. Solution for a fixed Mass Ratio γ

Let us first consider the case when we interested with the dependence $u_{cr} = f(\gamma)$, i.e. where the mass of the pipe and the mass of the fluid are given. In other words, the parameter γ is fixed as an input. A computer routine was developed to calculate the system eigenfrequencies for increasing values of the fluid speed. For a zero value of the fluid speed, $u = 0$, all the eigenfrequencies of eq. (28) are purely imaginary. They correspond to natural frequencies of vibration of the pipe filled with non-flowing fluid. For increasing fluid speed the real part of the eigenfrequencies of eq. (28) starts to decrease ($\mathrm{Re}\,\omega_i < 0$) until one of them reaches the zero value for a non null value of the fluid speed, corresponding to the critical velocity u_{cr} (flutter).

The behaviour of the system for increasing fluid speed can be visualized by means of the Argand diagram where the position of the eigenvalues is represented in the complex ω-plane by using the fluid speed u as a parameter. In the Argand plot the free eigenfrequencies of vibration, corresponding to zero flow speed, are indicated with a black circles (○). A small black arrow is used to indicate the direction of the eigenfrequencies path for increasing speed u starting from the free vibration values. Finally, a black triangle is used to highlight the eigenfrequency branch that leads to flutter instability.

In Fig. 2(a)-(b) the Argand diagrams are presented for dimensionless mass parameters $\gamma = 0.38$ and $\gamma = 0.40$, respectively. For $\gamma = 0.38$, Fig. 2(a), it can be seen that increasing the fluid speed the system become unstable when the real part of the second eigenfrequency reaches zero value for a critical flow speed $u_{cr} = 8.683$. For $\gamma = 0.40$, as it can be seen from Fig. 2(b), the system becomes unstable because the real part of the third eigenfrequency reaches zero for $u_{cr} = 8.779$.

The system reaches flutter state vibrating as the system's second mode in the first case ($\gamma = 0.38$) or as vibrating as a third mode in the second case ($\gamma = 0.40$). In between these two values of the mass ratio there must exist a value for which there is a change in the flutter dominating mode.

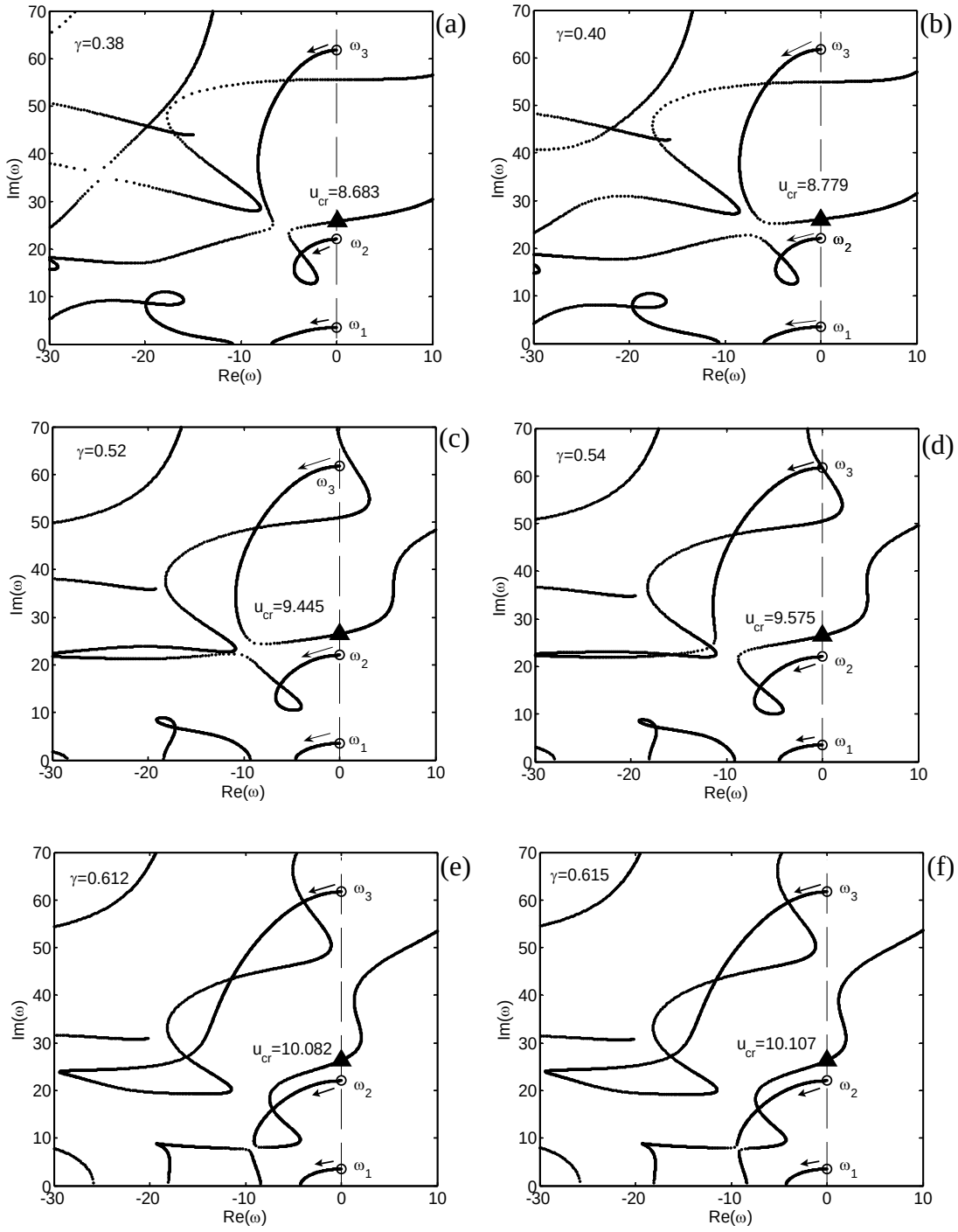

Fig. 2 - Argand diagrams for increasing values of the fluid speed u and for several values of the mass ratio: (a) $\gamma = 0.38$, (b) $\gamma = 0.40$, (c) $\gamma = 0.52$, (d) $\gamma = 0.54$, (e) $\gamma = 0.612$ and (f) $\gamma = 0.615$.

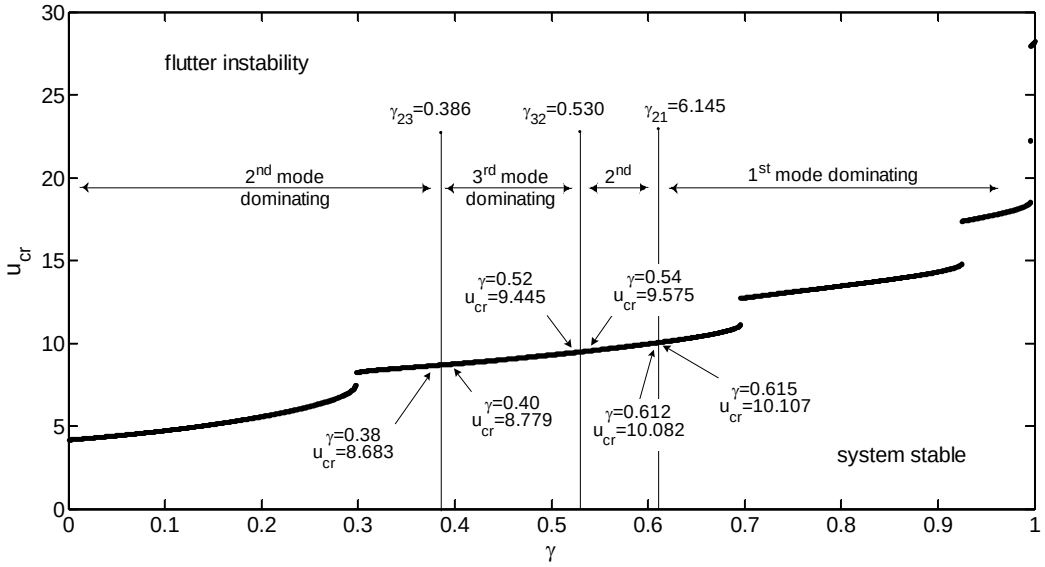

Fig. 3 - Critical flow speed versus the mass ratio parameter. Result obtained by sweeping over the fluid speed for a given value of the mass ratio parameter. The dominating mode of instability is highlighted.

In Ref. [16] this value denoted as γ_{23} was calculated as $\gamma_{23} = 0.386$. By increasing the mass ratio from γ_{23} up to unity other two changes of the flutter dominating mode are found: between $\gamma = 0.52$ ($u_{cr} = 9.445$) and $\gamma = 0.54$ ($u_{cr} = 9.575$) the dominating mode change from the third mode to the second mode takes place. Moreover, between $\gamma = 0.612$ ($u_{cr} = 10.082$) and $\gamma = 0.615$ ($u_{cr} = 10.107$) the dominating flutter mode switches from the second mode to the first one. These critical mass ratios corresponding to a change in the dominating flutter modes were calculated in Ref. [16] as $\gamma_{32} = 0.530$ and $\gamma_{21} = 0.6145$, respectively. The Argand plots for $\gamma = 0.52$, $\gamma = 0.54$, $\gamma = 0.612$ and $\gamma = 0.615$ are represented in Fig. 2(c)-(d)-(e) and (f), respectively. The plots in Fig. 2 perfectly match the results obtained in Ref. [16] demonstrating both the accuracy and reliability of the proposed GDQ solution technique.

At this point, an iterative computer routine was developed in order to evaluate the system critical flow velocity for increasing values of the fluid speed versus the mass ratio between zero to unity. The result is given in Fig. 3 where the relation between the dimensionless critical value u_{cr} and the mass ratio γ is presented along with the limits associated to the change in the dominating mode corresponding to flutter. Additionally, in Fig. 3 the critical fluid speed values for the six mass ratios that were examined in Fig. 2 via the Argand plane are indicated.

Clearly, critical flow speeds for values of the mass ratio close either to zero or unity are meaningless since $\gamma = 0$ corresponds to a system where the fluid has

zero mass, whereas $\gamma = 1$ is associated with the system where the pipe has a zero mass. Thus, the results in Fig. 3 can be viewed reliable in some sub-ranges as, $0.05 \le \gamma \le 0.95$ which corresponds to values of the mass of the pipe over the mass of the fluid between values $19 \ge m_p / m_f \ge 0.0526$.

In contrast of what was reported for years in several books and papers the stability map in Fig. 3 presents a monotonous behaviour with sudden jumps at some values of the mass ratio parameter. This discontinuous behaviour of the critical flow speed versus the mass ratio was recently reported by Elishakoff and Vittori [3]. However, in Ref. [3] these jumps appear for lower values of the mass ratio parameter compared to the ones obtained in this study. The reason of this discrepancy that will be explained later on in this study (Fig. 6(a) of section 4.2).

The critical fluid speed jumps can also be examined by means of the Argand plane. In Fig. 4(a) the Argand plane for a mass ratio parameter $\gamma = 0.296$ indicates that the system becomes unstable for zero value of the real part of the second eigenfrequency for a critical fluid speed $u_{cr} = 7.332$. In Fig. 4(b) a close up on the second eigenfrequency of Fig. 4(a) in proximity of the zero value of the real axis is portrayed. In addition, in Fig. 4(b) the second eigenfrequency branch for other two values of the mass ratio is given. For $\gamma = 0.296$ it can be seen that the lower part of the curve reaches zero value of the real axis for critical fluid speed $u_{cr} = 7.332$. For a value slightly bigger than the mass ratio $\gamma = 0.297$, the second eigenfrequency branch shifts a little to the left, reaches a zero value of the real axis for slightly increased path, and the critical fluid speed turns out to be $u_{cr} = 7.451$.

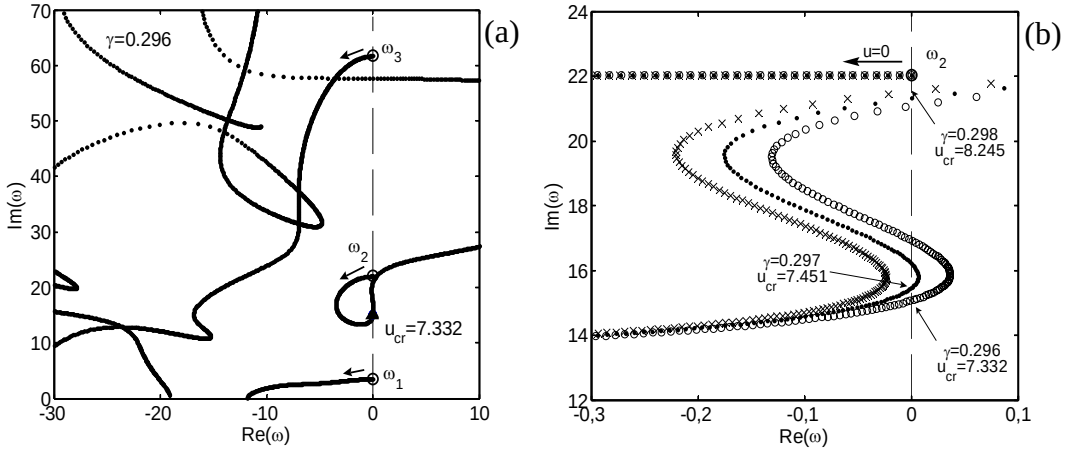

Fig. 4 - (a) Argand plane for a mass ratio parameter $\gamma = 0.296$. (b) Close up on the second branch close to the instability point for three different values of the mass ratio: $\gamma = 0.296$ (□□□□□), $\gamma = 0.297$ (•••••) and $\gamma = 0.298$ (×××××).

It can be seen that for a further increase of the mass ratio, $\gamma = 0.298$, the second branch shifts to the left sufficiently that it does not reach anymore the zero of the real axis in its lower part. For $\gamma = 0.298$, in fact, the second branch crosses the

zero value of the real axis on the Argand plane in its upper part with a much longer path corresponding to a critical flutter speed $u_{cr} = 8.245$. It is so evident that between $\gamma = 0.297$ and $\gamma = 0.298$ a jump in the stability map takes place.
A more detailed study reveals that the first three jumps in the stability map represented in Fig. 3 are characterized as follows: first jump occurs at $\gamma = 0.2972$ ($u_{cr} = 7.5135$) and $\gamma = 0.2973$ ($u_{cr} = 8.2347$), whereas the second jump takes place between $\gamma = 0.6953$ ($u_{cr} = 11.1555$) and $\gamma = 0.6954$ ($u_{cr} = 12.7336$). The third jump takes place between $\gamma = 0.9246$ ($u_{cr} = 14.8486$) and $\gamma = 0.9247$ ($u_{cr} = 17.3851$).

5. Solution for a fixed Flow Speed u

A stability curve can be obtained by solving eq. (28) as $\gamma_{cr} = g(u)$, i.e. searching for those values of γ that lead to flutter for a given values of the fluid flowing speed. The stability map in this case is represented in Fig. 5.

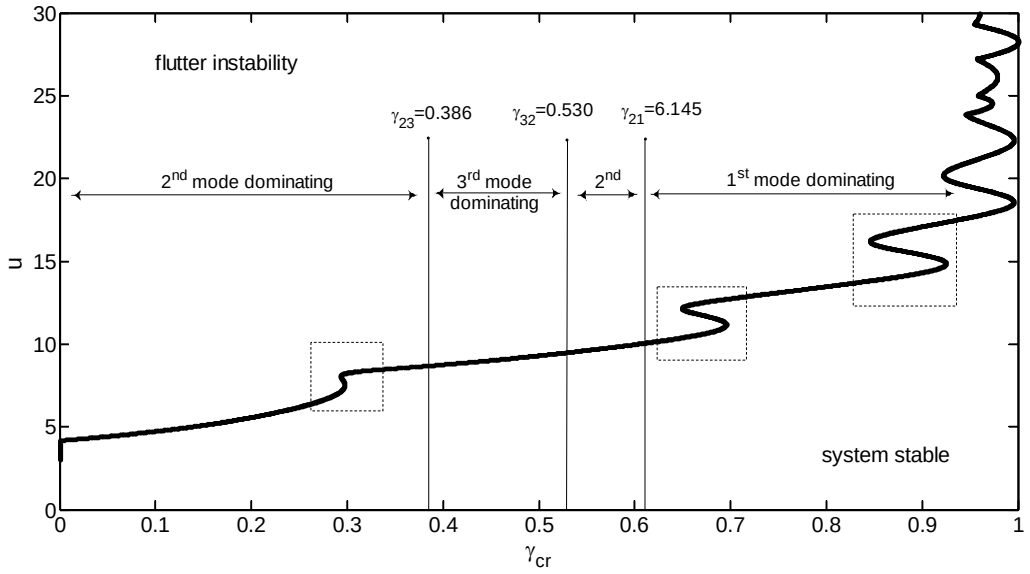

Fig. 5 - Critical flow speed versus the mass ratio parameter. Result obtained by sweeping over the mass ratio for a given value of the dimensionless fluid speed. The dominating mode of instability is highlighted.

The curve is continuous, in the sense that for each value of u in input there is a correspondent value γ_{cr} in output, and no jumps are present. Except for the very low $\gamma \le 0.05$ and very high $0.95 \le \gamma$ values of the mass ratio, where as stated before the solution is doubtful, this plot is in perfect agreement with the one given for example in Ryu et al. [16]. Clearly, the stability map in Fig. 5 include completely the stability map of Fig. 3, corresponding to solutions of the same

equation. The surprising outcome that sprouts by solving eq. (28) as $\gamma_{cr} = g(u)$ is that for a given system, i.e. for a fixed value of the mass ratio γ, in some ranges there can exist up to three critical fluid speeds. To observe this phenomena, see, for example, the three areas enclosed by a dashed square in Fig. 5.
In Fig. 6(a) a close up on the stability map for $0.29 \le \gamma_{cr} \le 0.30$ mass parameter, corresponding to the first area on the left of Fig. 5 rounded by a dashed square, is given. In this plot the solution obtained by solving eq. (28) as $\gamma_{cr} = g(u)$, in a continuous curve. It is overlapped with the solution obtained as $u_{cr} = f(\gamma)$, indicated by a sequence of black circles. The first jump values for the $u_{cr} = f(\gamma)$ solution are also highlighted in Fig. 6(a).
The existence of more than one critical fluid speed for a given mass ratio can be also seen via a sort of the Argand plane by using γ as parameter for a fixed fluid speed u.

In Fig. 6(b)-(c) and (d) the evolution of the frequencies of vibration for increasing values of the mass ratio parameter are given for a constant fluid speed $u = 7.0$, $u = 7.75$ and $u = 8.3$, respectively.

Let us to recall that these three last plots are not associated with a particular system; instead one considers the system that is changing continuously for a fixed value of the fluid speed. For example, in Fig. 6(b), for fluid speed $u = 7.0$, the frequencies of vibration for a system with $\gamma = 0$ are indicated by a black dot. One of this frequencies has a negative real part. This is because for $u = 7.0$ and $\gamma = 0$ the system is unstable flutter-wise since these $u - \gamma$ coordinates correspond to a point on the left side of the stability curve of Fig. 5.

By increasing the mass ratio the frequencies of vibration change. In the plot, a grey scale of colours has been used to indicate the mass ratio as increasing. In particular, an increasing mass ratio corresponds to a darker colour. It can be seen that the instability branch reaches the zero of the real axis for $\gamma_{cr} = 0.289$ corresponding to the critical mass ratio for $u = 7.0$. In fact, for a slightly greater mass ratio all the vibration frequencies have a negative real part corresponding to system stability.

A similar mathematical consideration can be done for the case of $u = 7.75$ in Fig. 6(c). It can be seen there that the system has a critical mass ratio $\gamma_{cr} = 0.2962$. Therefore, this mathematical result seems proving the existence of a critical flow speed $u = 7.75$ for a system characterized by a mass ratio $\gamma_{cr} = 0.2962$.

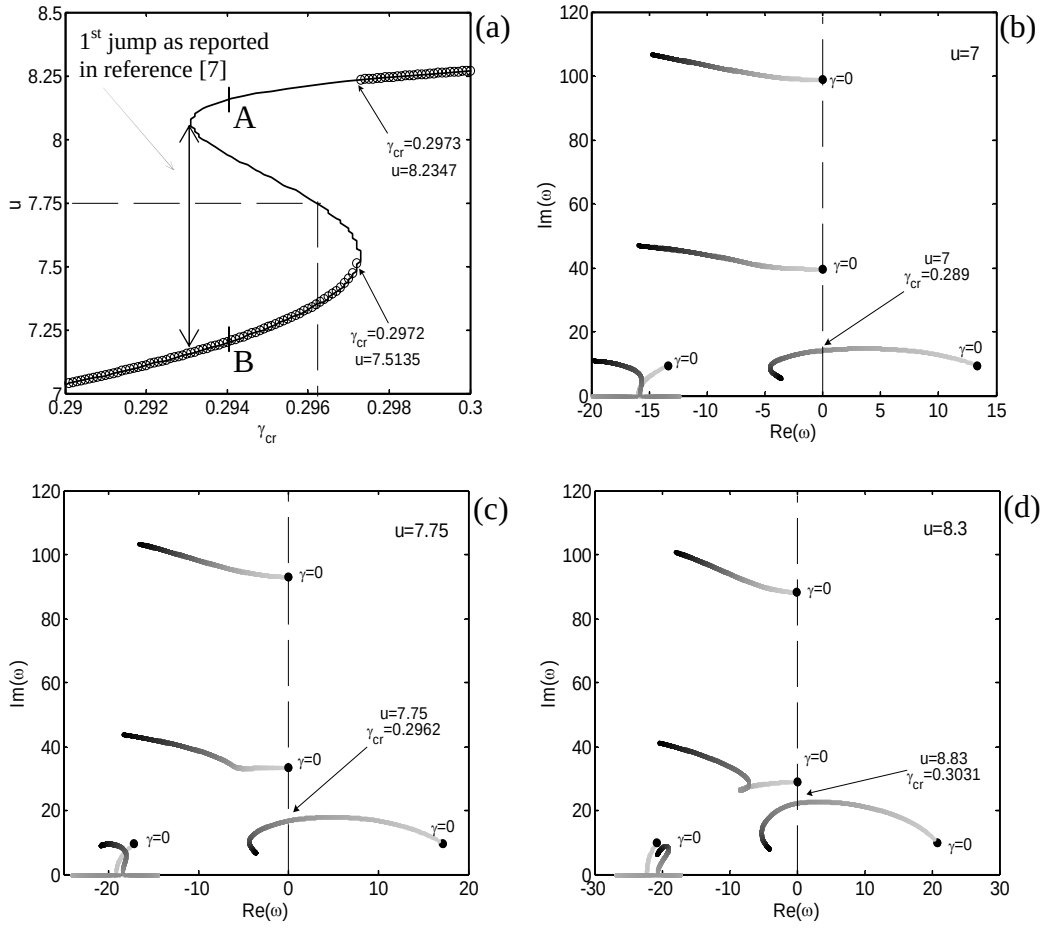

Fig. 6 - (a) Close up on the $0.29 \le \gamma_{cr} \le 0.30$ mass parameter range: $\gamma_{cr} = g(u)$ solution (———) overlapped to the $u_{cr} = f(\gamma)$ solution (∘∘∘∘∘). Frequencies of vibration for increasing values of the mass ratio parameter for a given constant fluid speed: (b) fluid speed $u = 7.0$, (c) $u = 7.75$ and (d) $u = 8.3$.

In Ref. [20], the first jump was found for a critical mass ratio $\gamma_{cr} \approx 0.2933$ compared to the one found in this paper that has the value of $\gamma_{cr} = 0.2972$. It appears that the authors of Ref. [3] while increasing the fluid speed looking for the solution (zero real part of the eigenfrequency) have not considered the smallest critical fluid speed. For example, in Ref. [20] the critical fluid speed for $\gamma = 0.294$ is found to be $u_{cr} = 8.122150$ while in this study the corresponding value is $u_{cr} = 7.2038$. The two values are indicated in Fig. 6(a) with the capital letters A and B, respectively.

The solution provided here was been carefully checked with the Argand diagram. A similar consideration holds for the others two jumps highlighted in Fig. 5 by dashed squares, for which the jump values in Ref. [3] were estimated at a lower mass ratio values.

6. Final Remarks

In this study the stability of a cantilever pipe conveying fluid is studied by means of the GDQ method. We conclude that this method can be conveniently used to perform parametric studies of stability of various pipes conveying fluid.
The paradoxical result of non-monotonic critical flow speed curve was investigated. The result is that by solving the stability problem as $u_{cr} = f(\gamma)$, i.e. looking for a critical flow speed for a given parameter γ, the stability curve presents a monotonic behaviour with jumps at particular values of the mass ratio. In contrast, by solving the problem as $\gamma_{cr} = g(u)$, i.e. searching for those critical mass ratio values for a given flow speed, the stability curve presents a well known non-monotonic behaviour in agreement with those presented in the literature during the years by many authors.

In order to verify experimentally this result, for a fixed fluid speed u, for example at $u = 7.75$, the mass ratio γ should be changed (by varying the mass of the fluid and/or the mass of the pipe) until an unstable behaviour is reached (γ_{cr}). It appears that it is practically more easily vary the mass of the fluid while keeping the pipe fixed. It is also worth noting that in the experimental procedure attention should be paid to the starting value for the mass ratio parameter γ. This values must be such to guarantee system stability (i.e. on the right side of the stability curve) for the assumed fluid speed. In our understanding, it is quite complicated to perform such an experiment for technical reasons, and up today no such an experiment is to be found in the literature. However, we trust that the definitive experiment of this kind will be performed by an inquisitive engineer(s) in order to provide the experimental side of the phenomena at hand.

On the other hand, the experiment could be easily performed for a given system, i.e. once the pipe and the fluid are defined, increasing the fluid speed starting from a zero value until the flow speed reaches the critical flow speed u_{cr} that leads to flutter. Once this speed is reached the system is unstable and a further increase of the fluid speed is meaningless. Experimentally, this seems to be the more logical although possibly not the only approach to trace the stability map for this problem.

Therefore, realistically, at a given value of γ only one critical flow speed can exist for the system, beyond of that the system is unstable for flutter, and the monotonic behaviour reported in Fig. 3 is the one representative of the physical aspect of the problem.

It appears that the well consolidated result reported in the literature regarding the non-monotonous stability curve for the pipe conveying fluid, should require an experimental validation in order to be definitely accepted.

Acknowledgments. This research was supported by the Italian Ministry for University and Scientific, Technological Research MIUR (40% and 60%). The research topic is one of the subjects of the Centre of Study and Research for the Identification of Materials and Structures (CIMEST) - "M. Capurso" of the University of Bologna (Italy). Professor Isaac Elishakoff appreciates partial support of the J.M. Rubin Foundation of the Florida Atlantic University.

References

[1] R.D. Blevins, Flow-Induced Vibration, Van Nostrand, New York, 1977.
[2] S.S. Chen, Flow-induced vibration of circular cylindrical structures, Chen Hemisphere Publishing Corp., Washington, D.C., 1987.
[3] I. Elishakoff and P. Vittori, A paradox of non-monotonicity in stability of pipes conveying fluid, Theoretical and Applied Mechanics, 32 (2005), 235-282.
[4] R.W. Gregory and M.P. Paidoussis, Unstable oscillation of tubular cantilevers conveying fluid. I-Theory, *Proceedings of the Royal Society of London. Series A, Mathematical and Physical Series*, 293(1435) (1966), 512-527.
[5] R.W. Gregory and M.P. Paidoussis, Unstable oscillation of tubular cantilevers conveying Fluid. II-Experiments, *Proceedings of the Royal Society of London. Series A, Mathematical and Physical Series*, 293(1435) (1966), 528-542.
[6] Y. Huang, G. Zeng and F. Wei, A new matrix method for solving vibration and stability of curved pipes conveying fluid, Journal of Sound and Vibration, 251 (2002), 215-225.
[7] N. Impollonia and I. Elishakoff , Does a partial foundations increase the flutter velocity of a pipe conveying fluid?", Journal of Applied Mechanics, 68 (2001), 206-212.
[8] G.L. Kuiper and A.V. Metrikine, On stability of a clamped-pinned pipe conveying fluid, Heron , 49 (2004), 1-22.
[9] S.I. Lee and J. Chung, New non-linear modelling for vibration analysis of a straight pipe conveying fluid, Journal of Sound and Vibration, 254 (2002), 313-325.
[10] Y.H. Lin and Y.K. Tsai, Nonlinear vibrations of Timoshenko pipes conveying fluid, International Journal of Solids and Structures, 34 (1997), 2945-2956.
[11] A. Marzani, F. Tornabene and E. Viola, Nonconservative stability problems via Generalized Differential Quadrature method, Journal of Sound and Vibration, 315 (2008), 176-196.
[12] L.G. Olson and D. Jamison, Application of a general purpose finite element method to elastic pipes conveying fluid, Journal of Fluids and Structures, 11 (1997), 207-222.

[13] H.R. Oz, Non-linear vibrations and stability analysis of tensioned pipes conveying fluid with variable velocity, International Journal of Non-Linear Mechanics, 36 (2001), 1031-1039.
[14] M.P. Païdoussis, *Fluid-Structure Interactions: Slender Structures and Axial Flow*, Vol. 1. Academic Press, London, 1998.
[15] Q. Qian, L. Wang and Q. Ni, Instability of simply supported pipes conveying fluid under thermal loads, Mechanics Research Communications, 36 (2009), 413-417.
[16] S.U. Ryu, Y. Sugiyama and B.J. Ryu, Eigenvalue branches and modes for flutter of cantilevered pipes conveying fluid, Computers and Structures, 80 (2002), 1231–1241.
[17] C. Shu, Differential Quadrature and its Application in Engineering, Springer, Berlin, 2000.
[18] F. Tornabene and E. Viola, Vibration analysis of spherical structural elements using the GDQ method, Computers and Mathematics with Applications, 53 (2007), 1538-1560.
[19] M. Vassilev and P.A. Djondjorov, Dynamic stability of viscoelastic pipes on elastic foundations of variable modulus, Journal of Sound and Vibration, 297 (2006), 414-419.
[20] E. Viola and F. Tornabene, Vibration analysis of damaged circular arches with varying cross-section, Structural Integrity & Durability (SID-SDHM), 1 (2005), 155-169.
[21] E. Viola and F. Tornabene, Vibration analysis of conical shell structures using GDQ method, Far East Journal of Applied Mathematics, 25 (2006), 23-39.
[22] E. Viola, M. Dilena and F. Tornabene, Analytical and numerical results for vibration analysis of multi-stepped and multi-damaged circular arches, Journal of Sound and Vibration, 299 (2007), 143-163.
[23] L. Wang and Q. Ni, In-plane vibration analyses of curved pipes conveying fluid using the generalized differential quadrature rule, Computers and Structures, 86 (2008), 133-139.

Received: July, 2009